THE GEOLOGICAL SOCIETY OF AMERICA®

Weathering and abrasion of bedrock streambed topography

Brendan P. Murphy[1,2]*, Joel P.L. Johnson[2], Nicole M. Gasparini[3], Gregory S. Hancock[4], and Eric E. Small[5]
[1]Department of Watershed Sciences, Utah State University, 5210 Old Main Hill, NR 138, Logan, Utah 84322, USA
[2]Department of Geological Sciences, The University of Texas at Austin, 2305 Speedway, Stop C1160, Austin, Texas 78712, USA
[3]Department of Earth and Environmental Sciences, Tulane University, 101 Blessey Hall, New Orleans, Louisiana 70118, USA
[4]Department of Geology, College of William and Mary, P.O. Box 8795, Williamsburg, Virginia 23187, USA
[5]Department of Geological Sciences, University of Colorado–Boulder, Campus Box 399, 2200 Colorado Avenue, Boulder, Colorado 80309, USA

ABSTRACT

Our framework for understanding morphodynamic feedbacks in bedrock rivers is built upon the assumption that rock erodibility is reasonably uniform at the sub-reach scale. Here, we demonstrate that climate-controlled rock weathering combined with bedload abrasion can produce systematic spatial variations in erodibility across bedrock streambed topography. Rock strength data from five channel reaches across the Big Island of Hawai'i show that upstream-oriented rock surfaces are stronger than downstream-oriented surfaces on the same bedrock protrusion. Moreover, the overall strength of these protrusions correlates with local mean annual precipitation rate, demonstrating climatic control of streambed erodibility. Comparing inferred field abrasion rates with experimental flume measurements, we demonstrate that abrasion rates scale exponentially with the orientation of local bed topography relative to streamflow, independent of weathering. However, the spatial variability in abrasion rate across bedrock protrusions is significantly reduced in the field, where large spatial variations in erodibility occur due to weathering. The methods presented here provide a straightforward field-based approach for evaluating the potential influence of weathering on abrasion in bedrock rivers.

INTRODUCTION

The recognition that climate, erosion, and tectonics are coupled has greatly improved our understanding of Earth surface evolution at regional and global scales (Willett, 1999). However, our ability to interpret these feedbacks is limited by a poor understanding of the mechanisms by which climate controls erosion (Perron, 2017). The denudation of steep, unglaciated landscapes is set by the incision rate of bedrock channels (Howard et al., 1994), which erode by some combination of abrasional wear, block plucking, weathering, and possibly cavitation (Whipple et al., 2000). The processes of weathering physically weaken rock (Aydin and Basu, 2005) and vary with local climate (Chadwick et al., 2003), providing a potential mechanism for the climatic control of bedrock river incision (Murphy et al., 2016).

Recent work has increasingly recognized the role of weathering in bedrock river erosion and channel morphology (Hancock et al., 2011; Small et al., 2015; Murphy et al., 2016; Shobe et al., 2017). Collectively, these studies found that competition between weathering (which weakens surficial rock) and erosion (which removes surficial rock, exposing stronger and less-weathered rock beneath) can produce systematic patterns of rock strength (i.e., erodibility) over spatial scales from channel cross sections to longitudinal profiles.

Here we explore interactions among weathering and abrasion at a smaller spatial scale: topographic protrusions (i.e., bed roughness features <≈1 m) along bedrock streambeds. Our study focuses on this scale because understanding morphodynamic feedbacks between streambed topography, streamflow, and sediment transport is critical for predicting the rates and patterns of erosion in bedrock rivers (Johnson and Whipple, 2010). Using new field data from the Big Island of Hawai'i and reanalyzing experimental data from Johnson and Whipple (2010), we test the following hypothesis: If chemical weathering weakens the streambed (e.g., Murphy et al., 2016) and bedload preferentially abrades upstream-oriented stoss faces of bedrock protrusions (e.g., Wilson et al., 2013), then bedload abrasion should remove weathered material on stoss surfaces, exposing less weathered bedrock from below, and stoss faces should be stronger than lee faces. Conversely, if weathering negligibly influences rock strength in the channel bed, then rock strength should be spatially uniform across bed topography. Our results demonstrate that the combination of climate-dependent weathering and bedload abrasion produces systematic, spatial patterns of bedrock erodibility at the scale of streambed roughness, establishing a link between climate and morphodynamic feedbacks in bedrock rivers.

FIELD AND EXPERIMENTAL METHODS

Erosional bedrock morphologies and corresponding rock strengths were measured in five basalt channel reaches across the Kohala Peninsula of the Big Island of Hawai'i. Due to an orographic rainfall gradient, mean annual precipitation (MAP) at the study reaches ranges from 280 mm/yr to 1840 mm/yr (Giambelluca et al., 2013) (Fig. 1A). Consistent with other first- and second-order channels in Kohala, as well as in other hydroclimatic regimes (e.g., Caruso, 2014), intermittent streamflow frequently exposes these streambeds to subaerial weathering processes. Additionally, with no quartz in this system, we observed little sand-sized sediment in the field available for suspension, suggesting that fluvial transport is dominated by washload and bedload.

While roughness features are common in bedrock channels, we selected reaches that had numerous bedrock protrusions with measurable "faces" (Fig. 1B). Here, "face" refers to a planar surface of bedrock that can be characterized by a single strike and dip over an area (≥200 cm^2) sufficient to collect a statistically significant number of replicate rock strength measurements. Protrusions were selected only if they had adequate upstream- (stoss) and downstream-oriented (lee) faces. In total, our data represent 48 faces on 23 features (one protrusion was large enough to collect two sets). Protrusions were smooth and rounded, suggesting that abrasion is the dominant erosion mechanism (e.g., Wilson et al., 2013) and that block plucking does not dominate the bedrock morphology here. Other than spatially variable color and strength, we observed no differing physical or lithologic heterogeneities between stoss and lee faces.

On each face, we collected 30 replicate, non-overlapping rock strength measurements using a type-N Schmidt hammer (Niedzielski et al., 2009). The Schmidt hammer measures the in situ elastic properties of rock (termed "rebound value", *RV*), which scale with rock compressive and tensile strength (Murphy et al., 2016). The spatial orientation of each face relative to flow was characterized by measuring the strike and dip as well as an azimuth characterizing the local average downstream flow direction (Figs. 1B and 1C).

*E-mail: bpmurphy@aggiemail.usu.edu

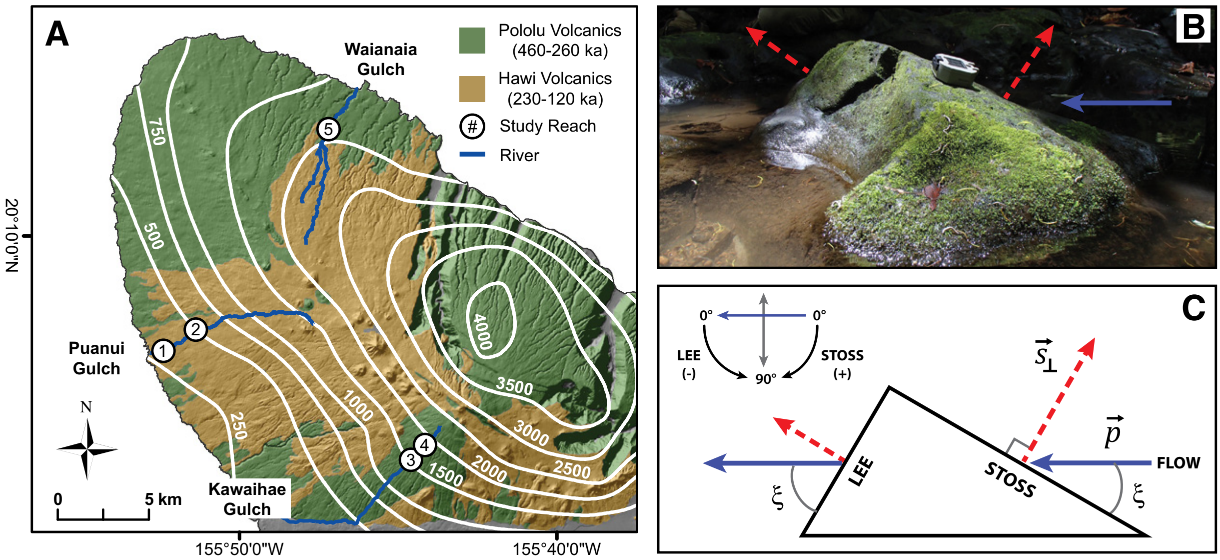

Figure 1. A: Map of Kohala Peninsula on Big Island of Hawai'i, showing our five field sites, basalt units (Wolfe and Morris, 1996), and isohyets of modern mean annual precipitation (MAP) in millimeters per year (Giambelluca et al., 2013). B: Photo of one bed protrusion annotated with lines of water and sediment flow direction (blue) and surface-normal vectors for stoss and lee faces (red). Brunton compass for scale. C: Cartoon of bed protrusion showing impact angle, ξ, surface-normal vectors, $\vec{s}_\perp$ (red), a horizontal flow and particle vector, $\vec{p}$ (blue), and the spatial reference system used for defining impact angles.

The angle at which bedload impacts the bed affects its imparted kinetic energy and is a critical control on abrasion rate (Huda and Small, 2014). It is impossible to constrain the trajectories of past impacts, so we assume that, on average, sediment movement is horizontal and parallel to the flow of water (Fig. 1C). The bedload impact angle, ξ, is then defined as: $90° - \cos^{-1}(\vec{p} \cdot \vec{s}_\perp)$, where $\vec{s}_\perp$ is the surface-normal vector, $\vec{p}$ is the particle trajectory vector, and values of ξ are positive for stoss faces and negative for lee faces.

To evaluate how abrasion rates vary across bed roughness features in the absence of weathering, we reanalyze data from the "bedrock" abrasion experiments of Johnson and Whipple (2010), in which the bed substrate was weak concrete with spatially uniform strength. The present analysis only evaluates runs with 100% bedrock exposure (runs 7–18; see Johnson and Whipple, 2010, their table 1) to isolate the effect of topography and eliminate the influence of alluvial cover (Sklar and Dietrich, 2001). While sediment mass flux remained constant during these runs, both discharge and median grain size (D_{50} = 2.7 and 5.5 mm) varied. We reanalyze topographic data collected along the centerline of the inner channel of the flume (subset shown in Fig. 2). Following Johnson and Whipple (2010), we calculate erosion as the vertical change in elevation between sequential surveys. Assuming that average particle motion is horizontal, we characterize impact angle as the local bed slope.

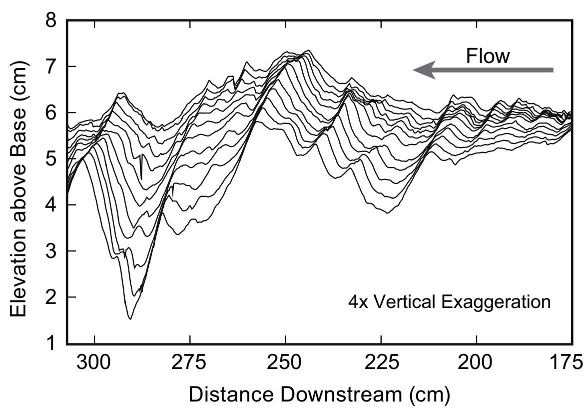

Figure 2. Section of inner channel topographic surveys from experimental runs 7–18 by Johnson and Whipple (2010). Full length profiles used in our analysis are shown in Figure DR2 (see footnote 1).

RESULTS

Experimental Abrasion

We find that the majority of abrasion (62%) in the experimental flume occurred on stoss faces, even though the distribution of all bed slopes is roughly normal (Fig. DR4 in the GSA Data Repository[1]). This distribution of erosion is characteristic of bedload abrasion, as opposed to suspended sediment abrasion (Whipple et al., 2000; Wilson et al., 2013). Quantitatively, the relation between experimental abrasion rate and impact angle is well fit by a weighted exponential function (blue line in Fig. 3; $R^2 = 0.93$). Rates were normalized by the average abrasion rate for the respective experimental run to account for variations in experimental conditions (i.e., grain size and discharge). These results establish the spatial relationship expected for local abrasion by bedload impacts over varying topography in the absence of weathering.

Field Rock Strength

At every field site and on every protrusion measured, the average rock strength, $\overline{RV}$, of stoss faces is stronger than that of lee faces (Fig. 4). Linear regression of $\overline{RV}$ against impact angle for the entire data set indicates a weak but positive relationship ($R^2 = 0.28$, $p < 0.0002$), but correlations improve for site-specific linear regressions (Fig. 4A; $R^2 = 0.35–0.98$; Table DR2 in the Data Repository), suggesting systematic variations between reaches. First, we find $\overline{RV}$ of the faces is negatively correlated with local MAP at each site (Kendall's rank correlation coefficient (τ) = −0.4, $p <$ 0.0003), suggesting that climate-dependent chemical weathering modulates erodibility, as demonstrated regionally by Murphy et al. (2016).

[1]GSA Data Repository item 2018154, field setting, controls on weathering and rock strength, field methods, and methods of data analysis; supplemental figures (complete flume profiles, histograms of field and flume data, and all field and flume abrasion rates); supplemental tables (orientation and average rebound value for each face, binned statistics from Figure 3, and regression parameters from Figure 4A), is available online at http://www.geosociety.org/datarepository/2018/ or on request from editing@geosociety.org.

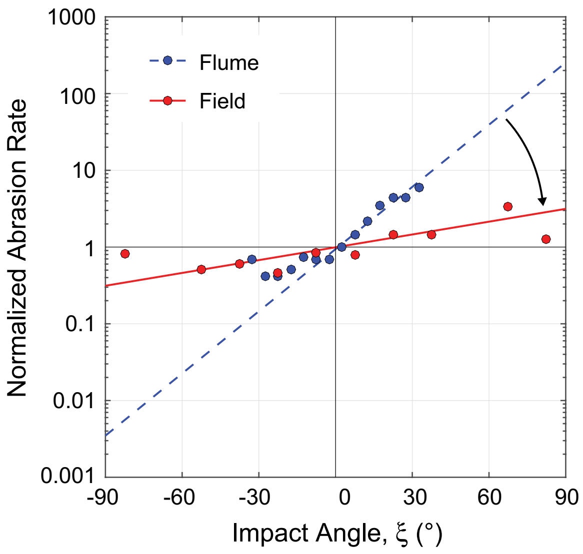

Figure 3. Comparing binned averages of normalized abrasion rates for field and flume data with impact angle (ξ). Red line shows best-fit weighted exponential regression to field data, where normalized abrasion rate is 0.94exp(0.012ξ) (R^2 = 0.69). Blue dashed line shows best-fit weighted exponential regression to flume data, where normalized abrasion rate is 0.9exp(0.064ξ) (R^2 = 0.93). Both regressions are extrapolated through full range of impact angles. Black arrow indicates proposed effect of weathering on the distribution of abrasion rates with impact angle. See the Data Repository (see footnote 1) for figures showing all data.

However, abrasion also modulates rock strength by removing weathered material. Although we cannot measure long-term abrasion rate at the scale of protrusions, variability in $\overline{RV}$ from site-specific regressions or from the climate trends, such as at site 3 (Fig. 4A), likely represents variations in abrasion due to localized variability in bed shear stress, sediment flux, or frequency of abrasional events (see the Data Repository).

To account for such variations and to isolate the effect of impact angle on strength, we normalize $\overline{RV}$ by dividing the average strength of each face by the average strength of the entire respective protrusion (i.e., average of stoss and lee): $\overline{RV}_{\text{norm}} = \overline{RV}_{\text{face}} / \overline{RV}_{\text{protrusion}}$. On every feature, the normalized strength data demonstrate that lee faces are weaker (<1) than their corresponding stoss faces (>1) (Fig. 4B).

Field Abrasion

It was not possible to directly measure abrasion rates across protrusions at our field sites. To compare experimental and field data, we instead calculate abrasion rates for protrusion faces using a relationship empirically derived by Murphy et al. (2016) that relates reach-averaged rock strength and climate across Kohala to long-term channel downcutting:

$$\overline{RV} = 10^{2.97} P^{-0.34} I^{0.32}, \tag{1}$$

where P is local MAP (m/yr) and I is incision rate (m/yr). Rearranging Equation 1, we use measured $\overline{RV}$ and solve for I. One limitation to this approach is that if abraded rock has the same strength as unweathered rock, then inferred abrasion rates could be underestimated. However, unweathered Kohala basalts have $\overline{RV} \approx 70$ (Murphy et al., 2016), and all the faces we measured have $\overline{RV} < 62$, suggesting that it is unlikely that abrasion rates are great enough to remove all weathered material.

As with the experimental data, the relationship between impact angle and abrasion rate for the field data is well fit by a weighted exponential function (red line in Fig. 3; $R^2 = 0.69$). Abrasion rates were normalized by the average of all abrasion rates calculated for each reach to account for variations in reach-averaged conditions (e.g., flow regime, sediment flux, climate, weathering rate). Importantly, the field data (with its spatially variable erodibility) exhibits abrasion rates with a significantly weaker dependence on impact angle than the flume data. Extrapolating the field data regression suggests that stoss faces oriented normal to flow (ξ = 90°) would have an abrasion rate 2.7× greater than surfaces oriented parallel to flow (ξ = 0°). In the flume, the same relative difference in abrasion rate would be 293× (Fig. 3).

DISCUSSION AND CONCLUSIONS

Independent of local climate and abrasion conditions, every stoss face we measured was stronger than its respective lee face (Fig. 4B), consistent with our hypothesis that weathering influences bedrock river erodibility. These variations in strength across bed roughness features translate to

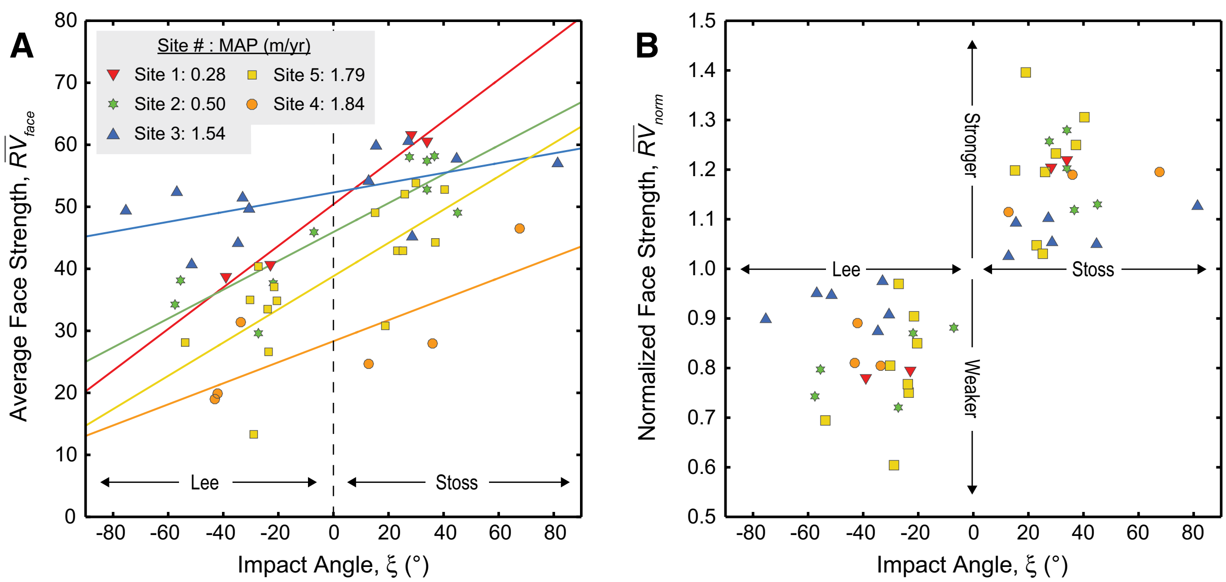

Figure 4. Field measurements of rock strength for 48 faces across five field sites at Kohala Peninsula on Big Island of Hawai'i. A: Average (n = 30) rebound value for each face, $\overline{RV}_{\text{face}}$, with impact angle, ξ. Color of regressions corresponds to symbol color for each site. MAP—mean annual precipitation. B: Normalized rebound values, $\overline{RV}_{\text{norm}}$, plotted with impact angle. Linear regression of all faces produces statistically significant relation: $\overline{RV}_{\text{norm}}$ = 0.004ξ + 1.0 (R^2 = 0.64, p < 0.02).

large differences in erodibility: rock erodibility scales nonlinearly with rock strength (Sklar and Dietrich, 2004). Accordingly, we find up to 20-fold differences in erodibility between stoss and lee faces on the same protrusion. Comparing the strongest stoss and weakest lee face measured from all of our sites, the relative difference in fluvial bedrock erodibility across this landscape is >300× (see the Data Repository).

However, erodibility does not equal erosion. Both the field and flume data show that, independent of weathering, abrasion rate increases exponentially as surfaces are oriented more upstream relative to bedload impacts. While nonlinearity between abrasion rate and surface orientation has previously been recognized (e.g., Beer et al., 2017), our results (using two independent data sets) show that this relationship is exponential—validating a relation only previously suggested by numerical modeling (Huda and Small, 2014). Despite the many differences between experiments, numerical models, and our field data, the similarity in functional form between abrasion rate and surface orientation establishes a quantitative framework for future morphodynamic modeling of bedrock channel topography.

The influence of weathering on fluvial abrasion is highlighted by the differing regressions between the field and flume abrasion rates with bed orientation. In the absence of weathering, the exponential scalar for flume abrasion rates (0.064) is ~5× greater than for the field data (0.012) (i.e., regression slopes in Fig. 3). Abrasion rate is a function of both the cumulative kinetic energy of impacts and rock erodibility (Sklar and Dietrich, 2004), and bedload impacts are more infrequent and of lower energy on lee faces than stoss faces (Wilson et al., 2013; Huda and Small, 2014). However, if the spatially variable erodibility that develops due to weathering and abrasion, as our data show, is great enough, then lee faces could abrade at rates similar to those of stoss faces, despite infrequent, low-energy impacts. Weathering could then offset the spatial pattern of abrasion that occurs due to topography alone, and relax the dependence of abrasion rate on bed orientation (Fig. 3). Therefore, we propose that increases in weathering should lead to increasingly uniform distributions of bedload abrasion rate across streambed topography.

Systematic spatial variations in rock erodibility produced by weathering and abrasion should influence the evolution of streambed roughness topography and the morphodynamic feedbacks that control the rates and patterns of bedrock river erosion. As rivers adjust to steady-state topography, spatial or temporal variations in bed roughness could cause changes in river width or slope (Finnegan et al., 2005). Therefore, if climate-dependent weathering acts to either promote or diminish topographic roughness, then weathering and abrasion feedbacks at the scale of individual protrusions could play a role in the climatic imprint on bedrock rivers. The morphodynamic impacts of weathering on the evolution of streambed topography and the potential spatial relationships between climate, bed roughness, and river geometry warrant further investigation.

The final contribution of this study is methodological: comparing Schmidt hammer measurements of stoss and lee faces provides a straightforward and inexpensive field method for evaluating the potential influence of weathering in bedload-dominated bedrock rivers. If large differences in strength are observed between stoss and lee faces, then we posit that weathering processes may be affecting rock erodibility and should be considered. For field sites with calibrated relations among climate, rock strength, and abrasion (e.g., Equation 1), we also demonstrate that it is possible to use field measurements of rock strength to roughly constrain patterns and rates of bedrock river incision.

ACKNOWLEDGMENTS

This work was supported by the Ronald K. DeFord Field Scholarship and a National Science Foundation (NSF) Graduate Research Fellowship to Murphy, NSF grant EAR-1024982 to Johnson, and NSF grant EAR-1025055 and a Tulane Research Enhancement grant to Gasparini. We thank landowners Kohala Institute at ʻIole, Ponoholo Ranch, and Parker Ranch for continued access and support; L. Sklar, D. Mohrig, and D. Breecker for their thoughtful comments; and K. Murphy for his assistance in the field.

REFERENCES CITED

Aydin, A., and Basu, A., 2005, The use of Brazilian test as a quantitative measure of rock weathering: Rock Mechanics and Rock Engineering, v. 39, p. 77–85, https://doi.org/10.1007/s00603-005-0069-0.

Beer, A.R., Turowski, J.M., and Kirchner, J.W., 2017, Spatial patterns of erosion in a bedrock gorge: Journal of Geophysical Research: Earth Surface, v. 122, p. 191–214, https://doi.org/10.1002/2016JF003850.

Caruso, B.S., 2014, GIS-based stream classification in a mountain watershed for jurisdictional evaluation: Journal of the American Water Resources Association, v. 50, p. 1304–1324, https://doi.org/10.1111/jawr.12189.

Chadwick, O.A., Gavenda, R.T., Kelly, E.F., Ziegler, K., Olson, C.G., Elliott, W.C., and Hendricks, D.M., 2003, The impact of climate on the biogeochemical functioning of volcanic soils: Chemical Geology, v. 202, p. 195–223, https://doi.org/10.1016/j.chemgeo.2002.09.001.

Finnegan, N.J., Roe, G., Montgomery, D.R., and Hallet, B., 2005, Controls on the channel width of rivers: Implications for modeling fluvial incision of bedrock: Geology, v. 33, p. 229–232, https://doi.org/10.1130/G21171.1.

Giambelluca, T.W., Chen, Q., Frazier, A.G., Price, J.P., Chen, Y.-L., Chu, P.-S., Eischeid, J.K., and Delparte, D.M., 2013, Online Rainfall Atlas of Hawaiʻi: Bulletin of the American Meteorological Society, v. 94, p. 313–316, https://doi.org/10.1175/BAMS-D-11-00228.1.

Hancock, G.S., Small, E.E., and Wobus, C., 2011, Modeling the effects of weathering on bedrock-floored channel geometry: Journal of Geophysical Research, v. 116, F03018, https://doi.org/10.1029/2010JF001908.

Howard, A.D., Dietrich, W.E., and Seidl, M.A, 1994, Modeling fluvial erosion on regional to continental scales: Journal of Geophysical Research, v. 99, p. 13,971–13,986, https://doi.org/10.1029/94JB00744.

Huda, S.A., and Small, E.E., 2014, Modeling the effects of bed topography on fluvial bedrock erosion by saltating bed load: Journal of Geophysical Research: Earth Surface, v. 119, p. 1222–1239, https://doi.org/10.1002/2013JF002872.

Johnson, J.P.L., and Whipple, K.X, 2010, Evaluating the controls of shear stress, sediment supply, alluvial cover, and channel morphology on experimental bedrock incision rate: Journal of Geophysical Research, v. 115, F02018, https://doi.org/10.1029/2009JF001335.

Murphy, B.P., Johnson, J.P.L., Gasparini, N.M., and Sklar, L.S., 2016, Chemical weathering as a mechanism for the climatic control of bedrock river incision: Nature, v. 532, p. 223–227, https://doi.org/10.1038/nature17449.

Niedzielski, T., Migoń, P., and Placek, A., 2009, A minimum sample size required from Schmidt hammer measurements: Earth Surface Processes and Landforms, v. 34, p. 1713–1725, https://doi.org/10.1002/esp.1851.

Perron, J.T., 2017, Climate and the pace of erosional landscape evolution: Annual Review of Earth and Planetary Sciences, v. 45, p. 561–591, https://doi.org/10.1146/annurev-earth-060614-105405.

Shobe, C.M., Hancock, G.S., Eppes, M.C., and Small, E.E., 2017, Field evidence for the influence of weathering on rock erodibility and channel form in bedrock rivers: Earth Surface Processes and Landforms, v. 42, p. 1997–2012, https://doi.org/10.1002/esp.4163.

Sklar, L.S., and Dietrich, W.E., 2001, Sediment and rock strength controls on river incision into bedrock: Geology, v. 29, p. 1087–1090, https://doi.org/10.1130/0091-7613(2001)029<1087:SARSCO>2.0.CO;2.

Sklar, L.S., and Dietrich, W.E., 2004, A mechanistic model for river incision into bedrock by saltating bed load: Water Resources Research, v. 40, W06301, https://doi.org/10.1029/2003WR002496.

Small, E.E., Blom, T., Hancock, G.S., Hynek, B.M., and Wobus, C.W., 2015, Variability of rock erodibility in bedrock-floored stream channels based on abrasion mill experiments: Journal of Geophysical Research: Earth Surface, v. 20, p. 1455–1469, https://doi.org/10.1002/2015JF003506.

Whipple, K.X, Hancock, G.S., and Anderson, R.S., 2000, River incision into bedrock: Mechanics and relative efficacy of plucking, abrasion, and cavitation: Geological Society of America Bulletin, v. 112, p. 490–503, https://doi.org/10.1130/0016-7606(2000)112<490:RIIBMA>2.0.CO;2.

Willett, S.D., 1999, Orogeny and orography: The effects of erosion on the structure of mountain belts: Journal of Geophysical Research, v. 104, p. 28,957–28,981, https://doi.org/10.1029/1999JB900248.

Wilson, A., Hovius, N., and Turowski, J.M., 2013, Upstream-facing convex surfaces: Bedrock bedforms produced by fluvial bedload abrasion: Geomorphology, v. 180–181, p. 187–204, https://doi.org/10.1016/j.geomorph.2012.10.010.

Wolfe, E., and Morris, J., 1996, Geologic map of the Island of Hawaii: U.S. Geological Survey Miscellaneous Investigations Map I-2524-A, scale 1:100,000, 3 sheets, 18 p.

Manuscript received 25 September 2017
Revised manuscript received 19 February 2018
Manuscript accepted 25 February 2018

Printed in USA